Study of harmonic generation with a two-color field

Report
by
Elisavet Georgiadou

Lund Reports on Atomic Physics, LRAP-375

March 2007

Acknowledgment

First of all, I would like to address special thanks to Anne L'Huiller, that gave me the opportunity to work in her group and Olivier Guilbaud that was an excellent supervisor the whole time that we worked together, answering all the coming questions and explaining everything patiently.
Many thanks I owe to Marcus Dahlström, for his great help and interesting plots.
Finally, I thank Miguel Miranda and Florian Geier for sharing their LaTeX knowledge with me, as well as Emilie Pourtal for keeping the laser running.

Abstract

This work, done in the frame of a *Marie Curie Early Stage Research (ESR)* program, focused on the study of odd and even harmonic generation using a two color field (ω and 2ω).
An interferometer was built for this reason, nice data were taken under different conditions, as well as interesting conclusions were drawn, which are presented in the report.

Contents

Chapter 1

High Order Harmonic Generation

High order harmonic generation (HHG) occurs when intense femtosecond laser light interacts with atoms or molecules. Atoms respond highly non linearly to the strong laser field, emitting harmonics of high order, whose frequencies are odd multiples of the frequency of the incident laser field.

Most spectra have a very similar shape, displaying a regular decrease of the harmonic intensity for the first few orders, followed by a long spectral range, known as the plateau, where the harmonics have about the same intensities, up to a sudden and final drop, known as the cutoff, depicted in figure 1.1.

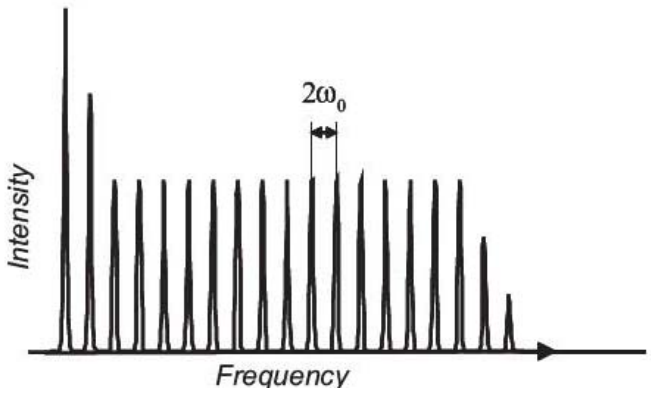

Figure 1.1: Harmonic generation setup

For symmetry reasons, high harmonics can be generated in linear polarization of the laser, but not in circular one. A way to understand it is to consider the atom in a frame rotating synchronously with the laser electric

field in circular polarization. The laser field is then seen as constant, so that a static response is induced, which yields an atomic response at the laser frequency only. As a result, the harmonics are usually linearly polarized, although they can also be elliptically polarized.

1.1 The three-step model

In media with inversion symmetry, like gas media, only odd harmonics are generated. This occurs simply because the atomic response is self-similar every laser half-cycle, but with a change of direction. In contrast, high harmonic generation on solid surfaces displays both odd and even harmonics, because there is no inversion symmetry on the surface.

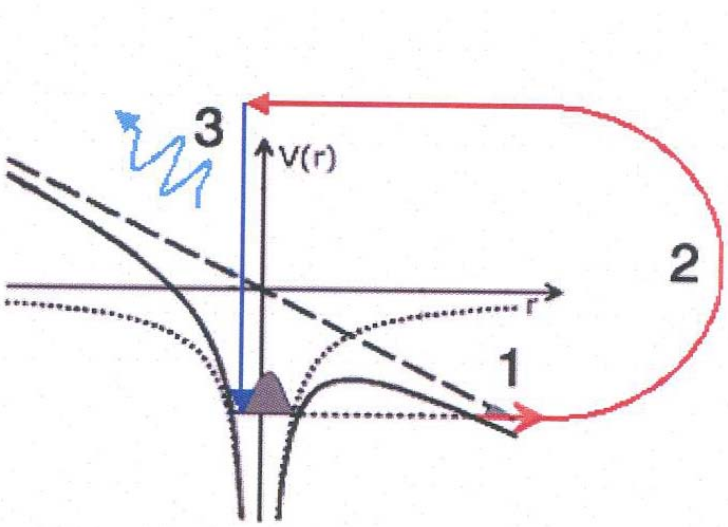

Figure 1.2: Schematic of the three step model

Several models have been proposed to explain the occurance of high order harmonics generated by individual atoms. The most successful one is the *three-step model* (or semi-classical model).
In this model the atomic potential is strongly distorted by the electric field of the laser (figure 1.2). When the external electric field is near maximum, the total potential of the atom and the laser field forms a barrier through which the electron may ionize by tunneling (1). When in the continuum, the electron is accelerated by the oscillating electric field, gaining kinetic energy (2). Finally, when the field changes sign, the electron may be accelerated back to the vicinity of the ion core where it recombines (3). When

the electron recombines, a photon, with energy equal to the one gained by the acceleration in the field plus the ionization potential, is emitted.

The amount of energy the electron could gain, I_p, depends on the phase of the electric field at the time of tunneling and the time of recombination. The maximum kinetic energy that the electrom could theoretically gain from the laser field is $3.2U_p$, where U_p is the ponderomotive energy, i.e. the average energy an electron can gain in an electric field. The ponderomotive energy is given by:

$$U_p = \frac{e^2 E_o^2}{4m\omega} \tag{1.1}$$

where e is the electron charge, E_o is the amplitude of the electric field, ω is the laser angular frequency and m is the electron mass. The total maximum photon energy, or the cut-off energy, is then $I_p + 3.2U_p$. All possible photon energies up to the maximum energy have approximately equal probability, leading to the long plateau of peaks of alomst equal amplitude, as mentioned before and shown in figure 1.1.
The reason that we get peaks at the harmonic frequencies and not just a continuum is because the process is periodic in time, since the electron tunnels out, when the electric field is close to the maximum. The fact that the process is periodic in time, also leads to a periodicity in frequency.
The period of this process is T/2, where T is the laser period. In an isotropic gas, no difference is observed when the electron tunnels out both when the electric field is -E and +E. This leads to a periodicity of 2ω in the frequency domain and only odd harmonics are observed.

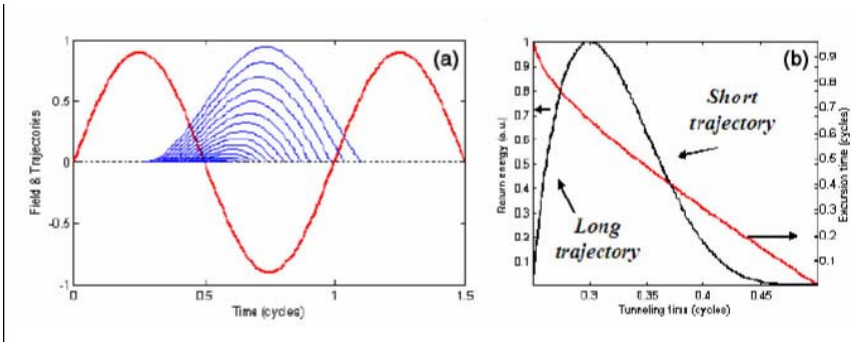

Figure 1.3: Schematic of the three step model

In this semi-classical model, a single electron is considered to accelerate along a certain trajectory, by the electric field of the laser (figure 1.3a), while in a quantum mechanical description, an ensemble of trajectories will

contribute to the wave packet. In figure 1.3b, the return energy of the electron along the excursion time, i.e time spent in the continuum is shown, as a function of the time at which the electron tunnels through the Coulomb barrier. When the electron recombines with its parent ion, a short burst of light is emitted. The properties of the emitted pulse are directly linked to those of the recolliding electron wave packet, making the temporal profile of the emitted light strongly dependent on the electron dynamics in the continuum. In figure 1.3b it is also shown that there are actually two different trajectories leading to each single return energy. The two trajectories differ in excursion time, leading to a significant difference in the properties of the emitted light.
Under most experimental conditions, the short trajectory is favoured by phase-matching conditions, making it dominate over the long trajectory.

To obtain odd and even harmonics, which is the goal of this work, the T/2 periodicity has to be broken. This can be achieved by mixing a small percentage of the second harmonic (2ω). Figure 1.4 shows the principle of high order harmonics generated with a two-color field. To the left side, one can see high order harmonics generated with one-color beam (ω), while to the right side, with both beams ($\omega + 2\omega$).

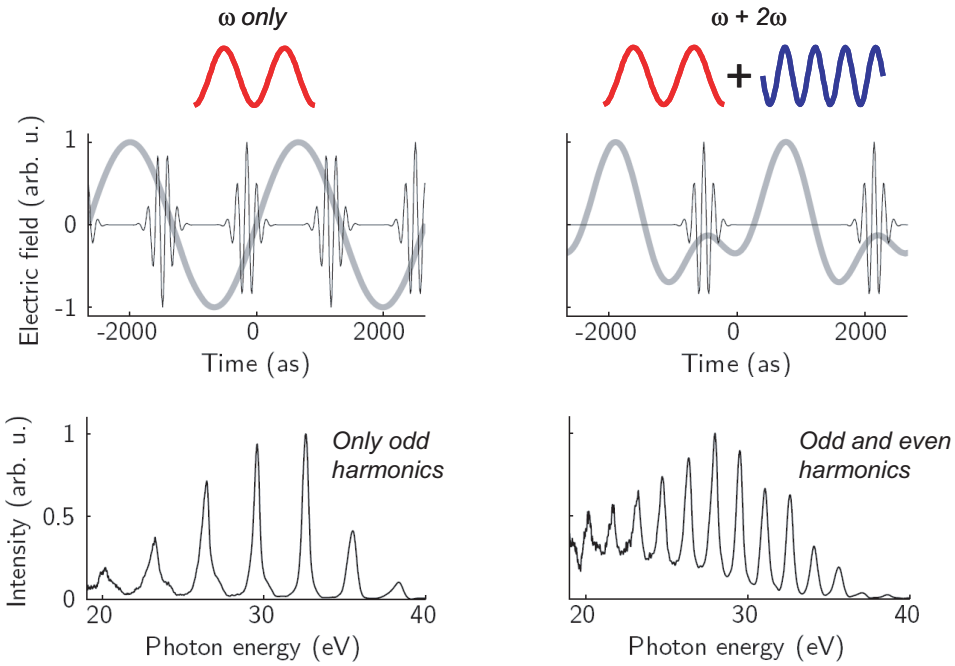

Figure 1.4: Schematic of the three step model

1.2 Phase matching

Phase matching is an important aspect of harmonic generation and when it is achieved, it means that the difference in phase between the induced polarization and the generated field is minimized over the medium length, leading to an efficient energy transfer from the laser field to the harmonics.

There are three main contributions that can result to phase shift between the incoming laser beam and the generated harmonics. The first one, *dispersion*, makes different frequencies travel with different velocities. The *Gouy phase shift*, second one, contributes when a laser beam is going through a focus and induces a geometrical phase mismatch. It can though be minimised, by using a loose focus and a short medium. Finally, the *intensity dependence of the harmonic dipole phase* also leads to an atomic phase mismatch. Studies of high order harmonics generated by a single atom exposed to an intense laser field, have shown that the dipole phase varies rapidly as a function of the laser intensity, especially for the long trajectory.

To explain phase matching, we consider second harmonic generation in the perturbative approximation. The laser field, in that case, can be writen as

$$E_1(z,t) = \frac{1}{2}[E_1(z)e^{i(k_1 z-\omega t)} + c.c.] \tag{1.2}$$

The laser field propagates in the medium and generates the second harmonic. The non-linear polarization then becomes

$$P_2^N L = \epsilon_o \chi^{(2)} E_1^2 = \epsilon_o \chi^{(2)} [E_1^2(z)e^{i(2k_1 z-2\omega t)} + c.c. \tag{1.3}$$

where $\chi(2)$ is the 2nd order susceptibility of the medium.
The emitted radiation has a wave vector k_2 and a frequency 2ω and the electric field at this frequency is

$$E_2(z,t) = \frac{1}{2}[E_2(z)e^{i(k_2 z-2\omega t)} + c.c.] \tag{1.4}$$

Comparing the polarization and the generated field, we can conclude that they will propagate with different phase velocities if there is a mismatch in wave vector, that is $k_2 \neq 2k_1$. The phase mismatch $\Delta k = k_2 - k_1$ has to be minimised in order to have an efficient energy transfer from the laser to the harmonics. The consequence of a lack of phase matching is given in figure 1.5.

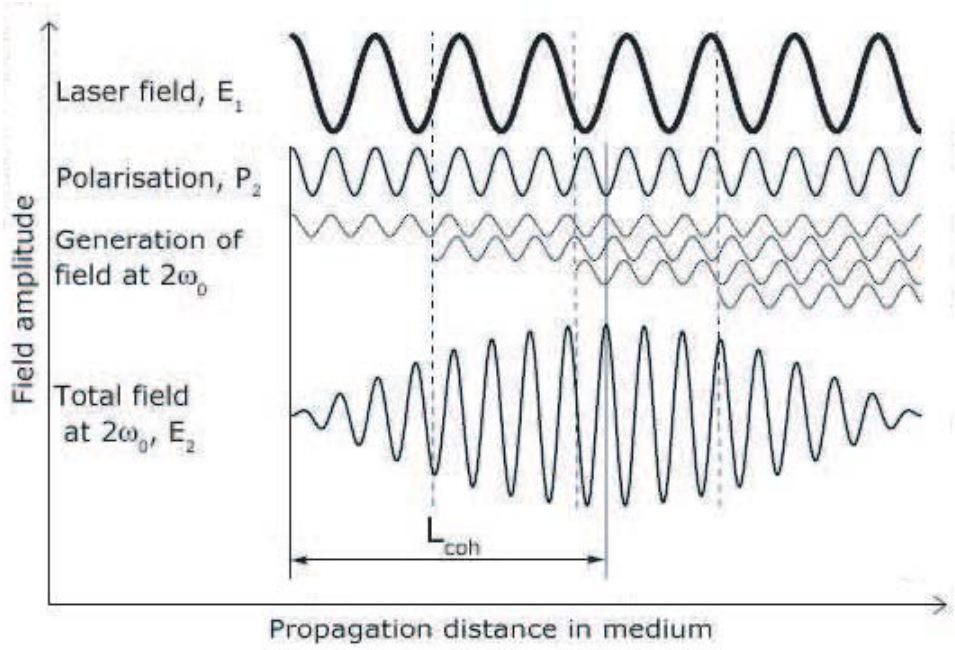

Figure 1.5: Effect of phase mismatch

A useful parameter characterizing phase matching is the *coherence length* L_{coh}, which is the distance for which the field is built up constructively. For a medium of length L_{coh}, two 2ω waves, emitted at the entrance and the end of the medium respectively, exit out of phase and cancel one another. L_{coh} is such, that $k_2 L_{coh}$ - $2k_1 L_{coh} = \pi$ that leads to

$$L_{coh} = \frac{\pi}{\Delta k} \tag{1.5}$$

When $\Delta k = 0$, phase matching is achieved and the conversion effciency increases with the medium's length. When $\Delta k \neq 0$, the energy transfer to the harmonics still occurs, but less efficiently (figure 1.5).

The long and the short trajectory both contribute to the harmonic dipole moment with a term characterized by a phase (Φ_i), given by

$$\Phi_i = -\alpha I(z) \tag{1.6}$$

The intensity dependent phase leads to spectral broadening and chirp of each harmonic. The coeficient α is different for the long (α_l) and short (α_s) trajectory and related to the time that the electron spends in the continuum. A longer excursion time corresponds to a larger α value. The spectral content and chirp of the harmonic will be quite different, according to which

trajectory is dominant. The intensity varies over the pulse temporally as well as spatially. The radial variation I(r) willl affect the curvature of the phase front of the harmonics, thus determining the divergence of the emitted beam. The short trajectory will be associated with a small divergence, whereas the long one leads to a large divergence. The total electric field of the generated harmonics can be written as

$$E = E_l e^{-i\alpha_l I} + E_s e^{-i\alpha_s I} \tag{1.7}$$

where E_l and E_s are the electric fields corresponding to the long and short trajectory, respectively. The square of the electric fields gives then the intensity of the harmonics.

Chapter 2

Experimental Setup

2.1 Harmonic generation setup

A scheme of the harmonic generation setup is presented in figure 1.2

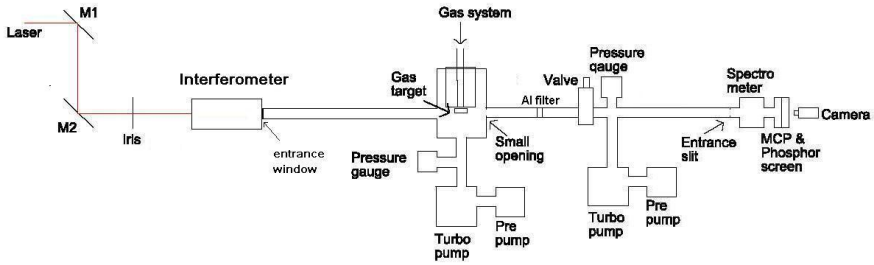

Figure 2.1: Harmonic generation setup

The experiment used the *Terawatt Laser* at the *Lund High Power Laser* facility at Lund University. The laser beam from the terawatt facility is sent to the experimental beam-line which is kept under vacuum to enable X-UV light to travel on long distances without significant absorption. The incoming IR laser beam (frequency ω) is first cut by an iris in order to get a defined, as well as variable, diameter of 1-2 cm. Then, by sending it to travel through a so-called ω-2ω *interferometer* (Interferometer in figure 2.1), 2ω frequency beam was generated and finally both beams were focused, by an off-axis parabolic mirror, into a gas target located in the interaction chamber. To minimize non linear effects, part of the beam, just after the focussing optics, is also kept under vacuum. A 200nm Al filter can be installed after the interaction chamber, as shown in figure 2.1, to eliminate the initial laser beam. Most of the results presented below, however, were obtained without.

A picture of the ω-2ω *interferometer*, as well as of the parabolic mirror setup, is presented in figure 2.2 and is schematized in figure 2.3.

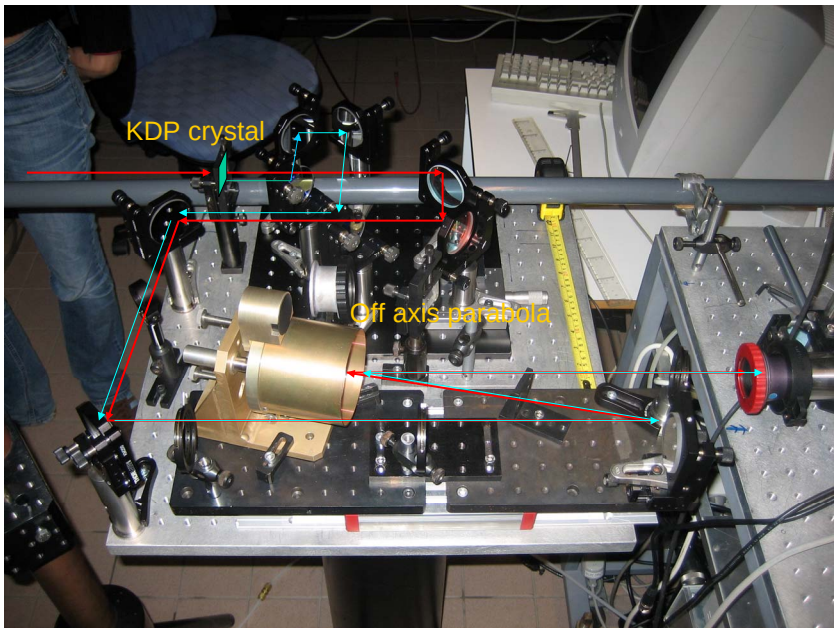

Figure 2.2: Interferometer and parabolic mirror setup

IRIS (mm)	ω (mJ)	2ω (mJ)	% $2\omega/\omega$
10	1.4	0.16	11.4
12	1.9	0.28	14.7
15	3	0.34	11.3

Table 2.1: Ratio $\omega/2\omega$ for june 15th experiments, when E_{jun15} (energy before compression) = 110 mJ

At the entrance of the interferometer (figure 2.2), the ω (red) beam, first travels through a Potassium DiDeuterium Phosphate (KDP crystal) of 700 μm thickness. Only a fraction of its energy, 10%, is converted to a double frequency blue beam (2ω) - table 2.1.

The two frequencies, ω and 2ω, are then separated by a dichroic beam splitter which allows the ω-beam (red line) to go straight through it, while the 2ω-beam (blue line) is reflected to a 90^0 angle and is following another path of the same distance. The two beams are recombined with the aid of a second beam splitter.

Using the parabolic mirror, we can to focus the initial (ω) beam as well as the generated (2ω) one to the same point. It is placed on a translation stage, in order to focus the beams in different positions with reference to the gas jet. Thus, the focal point can be either in the middle of the gas jet, a few cm before it or a few cm after it. The focal length of the mirror is 45cm. The results presented later with the reference z55 (or z30), have been obtained with the gas located after (before) the focus. Mirrors M1 and M2, in figure 2.1, are used for the alignment of the incoming laser beam.

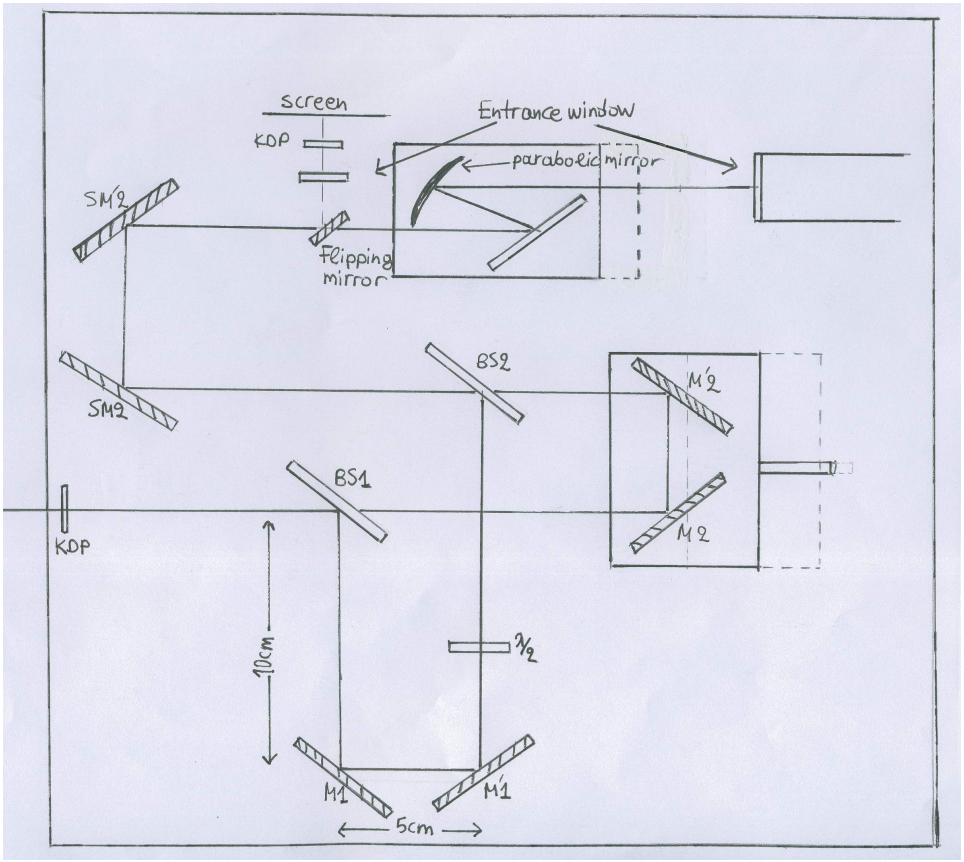

Figure 2.3: Scheme of the interferometer and the parabolic mirror setup

A very sensitive alignment is done to overlap the beams both in the spatial and temporal domains. Spatial overlapping was done by overlapping the beams both after the interferometer and far away.
Temporal overlapping was achieved first roughly by measuring the paths of the two beams and arranging them to be of the same length, by moving the translation stage on which the mirrors M2 and M2 are located (figure 2.3).For a more precise temporal overlapping, a small KDP crystal was

placed after the interferometer,with the aid of a flipping mirror, so that the 2ω beam passes through and a percentage of the ω beam is converted to 2ω. We move the translation stage of the ω path with small steps, of the order of some μm, until we observed interference fringes.

Both beams (ω and 2ω) are finally focused into the interaction chamber, by the parabolic mirror setup which properties are independent of the incoming wavelength. It is possible, with this device, either to let both beams to go to the HHG chamber so as to generate odd and even harmonics, or to select one of the two wavelengths to be directed to the HHG chamber, by blocking one of the two paths with a shutter, so as to create only odd, or even, harmonics of the IR frequency.

The use of ω and 2ω beams together, leads to generation of both odd and even harmonics.

2.2 The Multi-Terrawatt Laser System

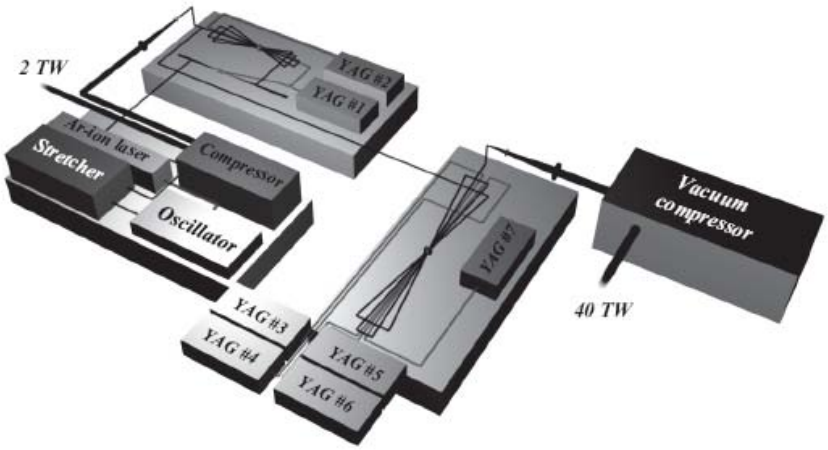

Figure 2.4: Terrawatt Laser System

The laser used in this work, is a powerful Ti:Saphire system and the pulses, amplified by the chirped pulse amplification technique, are compressed to 40fs duration at a wavelength of 800 nm and with energy up to 1J. The beam diameter is aproximately 4 cm and the pulse energy reaching our experimental setup was around 50 mJ (about 100 mJ before compression). A scheme of the Terrawatt Laser System is shown in figure 2.4.

2.3 The gas system

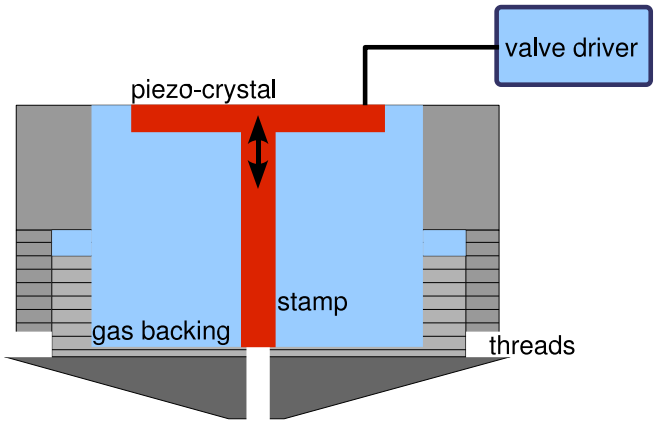

Figure 2.5: The gas system

The gas target (filled with Argon gas supplied by a tube) is installed in the middle of the interaction chamber. The release of the gas is made by a pulsed piezoelectric valve, as shown in figure 2.5. By applying a voltage on the piezo-crystal, the stamp moves up, the gas is released, with the aid of a jet nozzle, having a diameter of the order of 1mm and meets the laser beam. The control voltage is pulsed in order to supply a sufficiently high gas pressure, when the laser pulse arrives, while avoiding the increament of the background pressure in the chamber. The triggering valve opening was done by a valve driver that converts an electronic trigger signal, coming from the terrawatt laser, to a voltage pulse.

The nozzle position could be adjusted by micrometer screws in three directions. The laser beam was aligned as close as possible to the jet nozzle, because the radius of the gas jet is the smallest there and thus the density is the highest.

2.4 The Vacuum System

After focusing, the beam enters a tube (entrance window, figure 2.1), set before the gas jet, and travels in vacuum. This is necessary because the intensity of the beam is increased when it is focused. Thus nonlinear optical effects, like self-phase-modulation and self-focusing, would occur if travelling was done in the air. The beam profile would be distorted and the conditions for HHG would deteriorate. Furthermore, the generated harmonics have to be kept under vacuum in order not to be absorbed by the air. In the end, the MCP have to be pumped to a very low pressure (10^{-5}mbar).

Figure 2.6 shows a scheme of the vacuum system. The experimental setup is pumped by two different pumping systems, each one consisting of a primary pump as well as a turbomolecular pump. The first system is pumping directly under the gas jet to reduce the background pressure due to the pulsed noble gas. The pressure in this chamber, when the pulsed valve is operating, reaches a value of about 10^{-4}mbar. The other system is pumping before the spectrometer in order to achieve the lowest possible pressure for the MCP. The pressure here has to be around 10^{-5}mbar and it reaches values around 10^{-6}mbar after several hours of pumping.
A small aperture is placed after the gas jet to keep the gas flow to the second part (in lower vacuum) minimized.

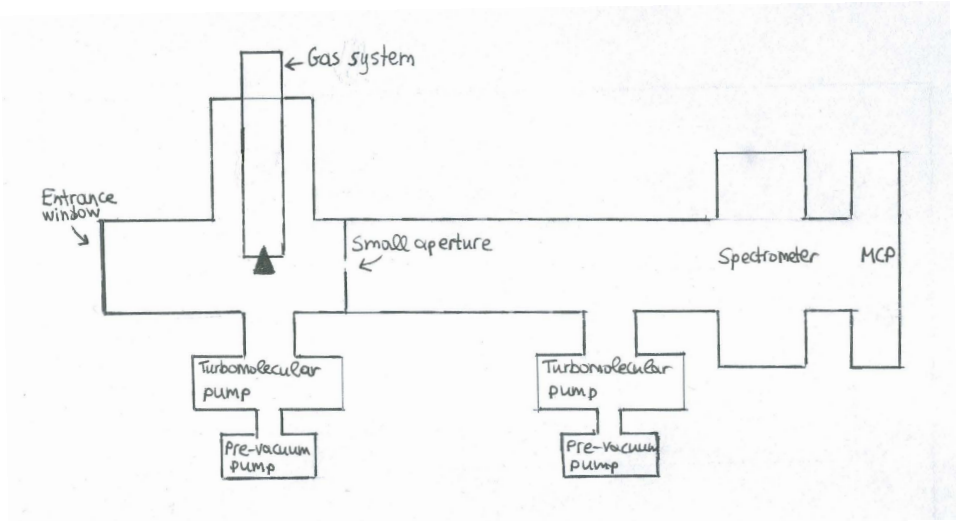

Figure 2.6: The vacuum system

2.5 The spectrometer

The spectrometer used is a flat filed I.S.A. Jobin-Yvon PGM PGS 200 spectrometer with a 200 μm entrance slit, located approximately 2m from the gas jet. It is composed of a toroidal mirror and a plane platinum coated grating. The grating, that has 450 grooves/mm, is designed for the spectral range of 16-80nm and separates different wavelength components. It can be rotated in order to detect different parts of the spectrum.

2.6 Detection

Micro-Channel Plates (MCP) were used, in our experiments, as a detector (figure 2.7). MCP consist of an array of 104-107 miniature electron multipliers channels, oriented parallel to each other having diameters of 10μm and spacing between them of 12μm. The channels have an angle of 8^o relative to the incident beam.
The electron multiplication takes place in the channels, under the presence of a strong electric field. Electrons, that travel in the channels, scatter frequently, producing secondary electrons. This process amplifies the original signal by several orders of magnitude, depending on both the strengh of the electric field and the geometry of the MCP.

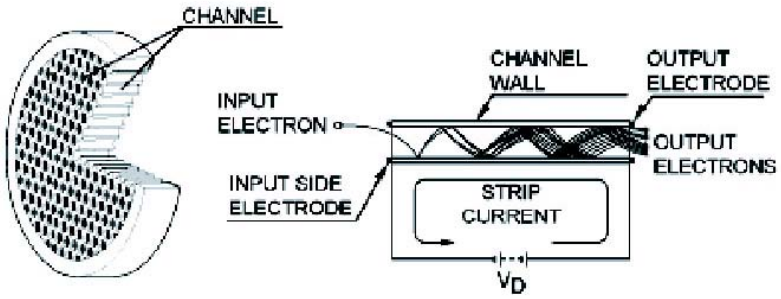

Figure 2.7: The Micro-Channel Plate (MCP)

A phosphor screen is used at the end to make the electron signal visible.
A final voltage of -1570 V was applied to the MCP, while the phosphor screen's final voltage was 3000 V. It is important to note that both of them reached their final voltages with an increament step of 100 V, starting with the phosphor's screen because it is crucial that its voltage is higher than the MCP's one, to prevent damaging of the MCP by "flying back" electrons (Apendix C). After hitting the screen, the electrons emit visible phosphorescent light.

2.7 CCD camera

A Charged-Coupled device (CCD) camera, type Marlin F-033B/C with 656×494 pixels, recorded the images produced on the phosphore screen. It was triggered by a signal from the laser and the recorded images were transfered to a computer.

The experimental work was done using 60 ms as recording time.

Chapter 3

Experiment

Harmonic generation with a two-color field (ω-2ω) took place with the experimental setup described in the previous chapter.

We tried to generate odd and even harmonics under different conditions and in the most efficient way. For that reason, we performed the experiment for different sizes of the ω and 2ω beams, different relative polarizations (parallel and cross) and different distances of the parabolic mirror from the gas jet, leading the beams to have focal points before, on, or after the gas jet.

To make the setup as stable as possible, as well as for safety reasons, we covered the interferometer and the parabolic mirror setup from the surroundings by a lock.

We also varied the delay between the ω and 2ω pulses. without observing much difference. We attribute this to small vibration of our setup and possibly a pointing instability of the laser.

3.1 Alignment

The alignment was first done without the parabolic mirror setup, to create a reference beam. Then it was repeated through the parabolic mirror setup, in which we adjusted the angle of the parabolic mirror (final angle with the direction of the reference beam 12.3^o) so as to make the beam passing through the center of the gas jet, from all possible positions of the translation stage.

The alignment testing was realized with the aid of a portable He-Ne laser and only in the end it was done with the laser beam coming from the Terrawatt laser facility.

3.2 Experimental results

1) In figure 3.1 typical example of experimental data is given.

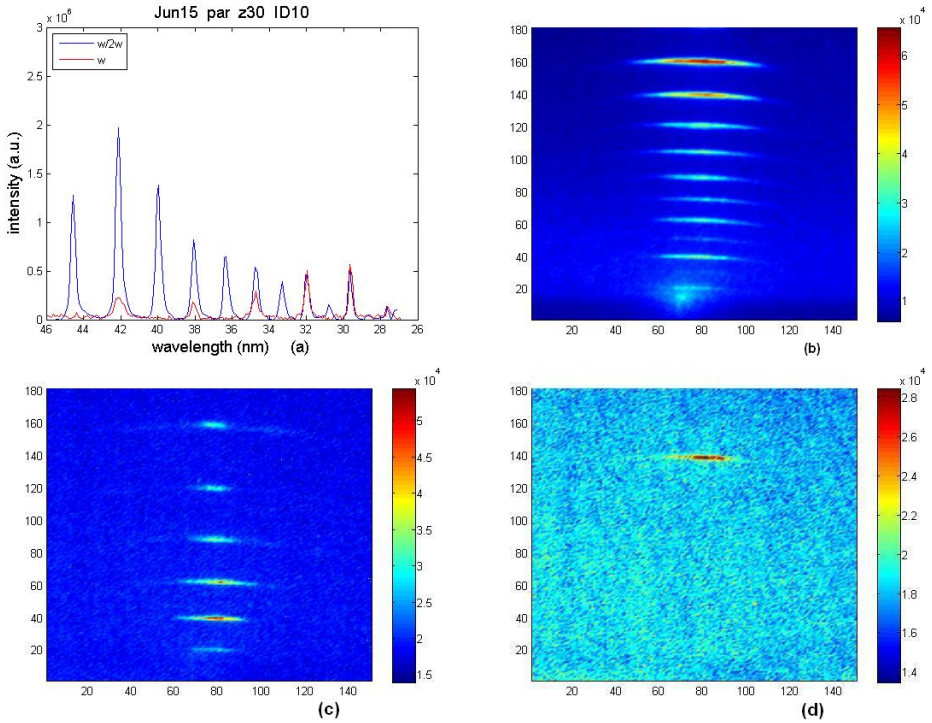

Figure 3.1: (a) specrta of ω and $\omega/2\omega$ harmonics, (b) color harmonic spectrum of the $\omega/2\omega$ beam, (c) color harmonic spectrum of the ω beam, (d) color harmonic spectrum of the 2ω beam

The name is giving information about the date as well as the conditions under which the experiment took place. So, in figure 3.1a, a plot of two spectra ($\omega/2\omega$, ω) is given. In $\omega/2\omega$ plot both ω and 2ω beams were directed to the gas jet, leading to odd and even harmonic generation, while in the ω plot the 2ω beam is cut and only odd harmonics are generated.

The part "par" of the name means that the laser beams had parallel polarization. Parameter "z" is giving the distance (in mm) of the parabolic mirror from the entrance window and in this particular example, the focal point of the beams is after tha gas jet (see section 2.1). The following number gives the iris (standing before the interferometer) diameter (ID) in mm. So, the size of the initial beam is prescribed. In figure 3.1b, 3.1c and 3.1d color spectra of the particular $\omega/2\omega$, ω and 2ω data respectively, are shown. The harmonics are quite clear, starting from high to low order from the bottom to the top of the figure.

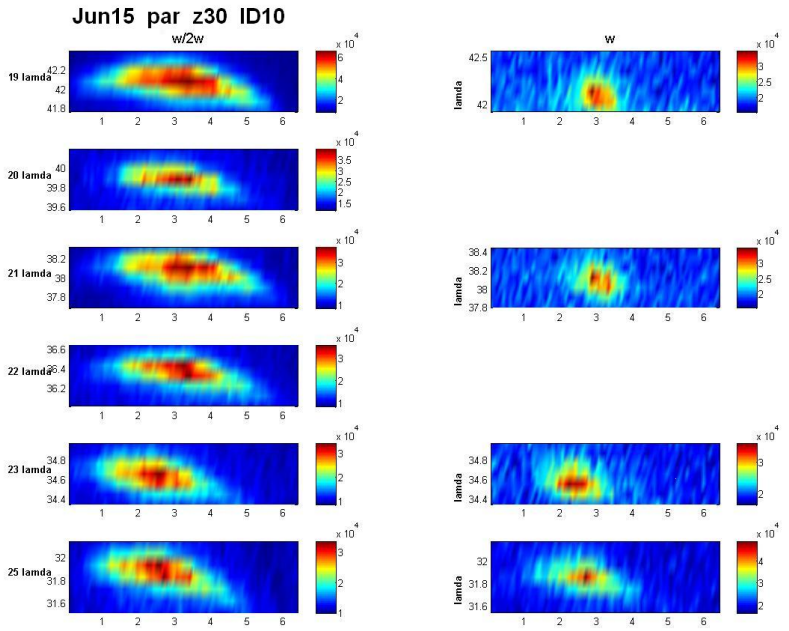

Figure 3.2: separate harmonics of the ω and $\omega/2\omega$ beams in divergence - wavelength axes

In figure 3.2 separate harmonics of the data file presented in figure 3.1 are shown. In these plots we show the divergence in mrad (x axis) versus the wavelength in nm (in y axis). The wavelength is calculated through the *lambda calibration* procedure (see Apendix A).
It is easily observed that the divergence of the $\omega/2\omega$ data is larger than with only ω.

2) Similar plots are given in figure 3.3, under different conditions. Here the focal point of the beams is before the gas jet (z55). In figure 3.3c, it is very easy to see the long and short trajectories and how they contribute to the harmonic generation. The long trajectory (as explained in section 1.2) is more divergent than the short one, which on the other hand is more intense. Very obvious long-short trajectory contribution can also be seen in figure 3.4c, with quite divergent harmonic lines but with lower intensity on the sides (long trajectory) compared to the intense middle part (short trajectory).
All the preceding color spectra are plotted with simple counters used in both axis.

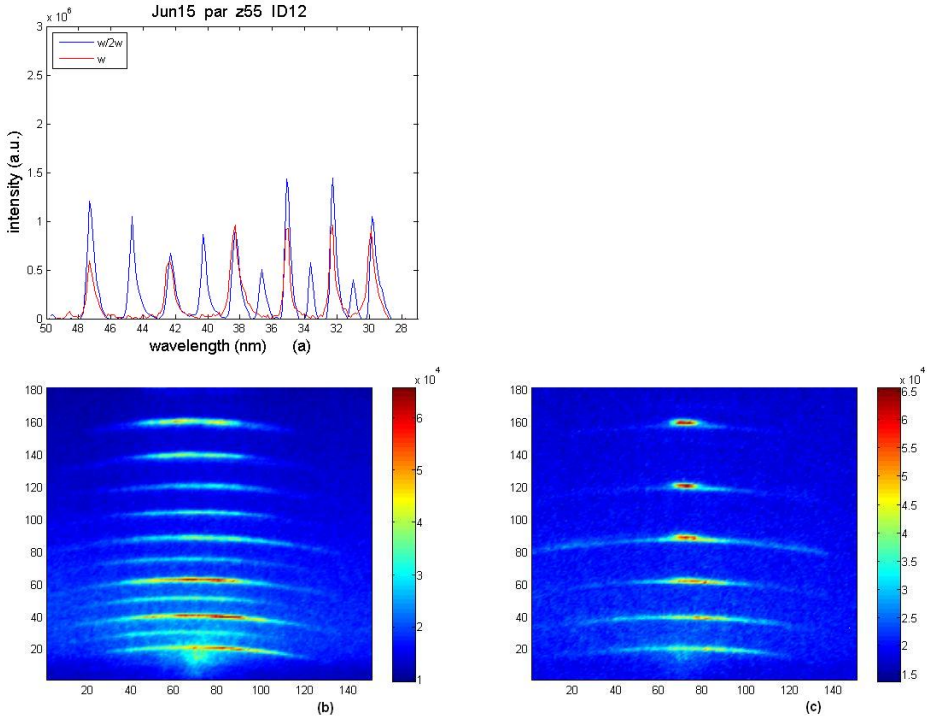

Figure 3.3: (a) specrta of ω and $\omega/2\omega$ harmonics, (b) color harmonic spectrum of the $\omega/2\omega$ beam, (c) color harmonic spectrum of the ω beam

3) In the plots of the figure 3.4 one can observe the influence of the position of the gas jet, described by the z parameter, to the appearance of the long trajectory.

4) In figure 3.5, the data were taken another day (June 29th), the focal point of the beams is after the gas jet (z30) and they are crossed polarized. A plot of an harmonic spectrum generated only from ω crossed polarized beam is presented in figure 3.6a. Comparatively to this, a spectrum taken under the same conditions and the same day with parallel polarization is presented in figure 3.6b. One can clearly see that the spectrum generated from the crossed polarized beam is much more intensed than the one taken with parallel polarization.

5) In the end, in figure 3.7, very interesting spectra are presented. A double structure is observed in all the plots. It is becoming, though, more clear as the size of the beam (defined by the iris diameter) increases.

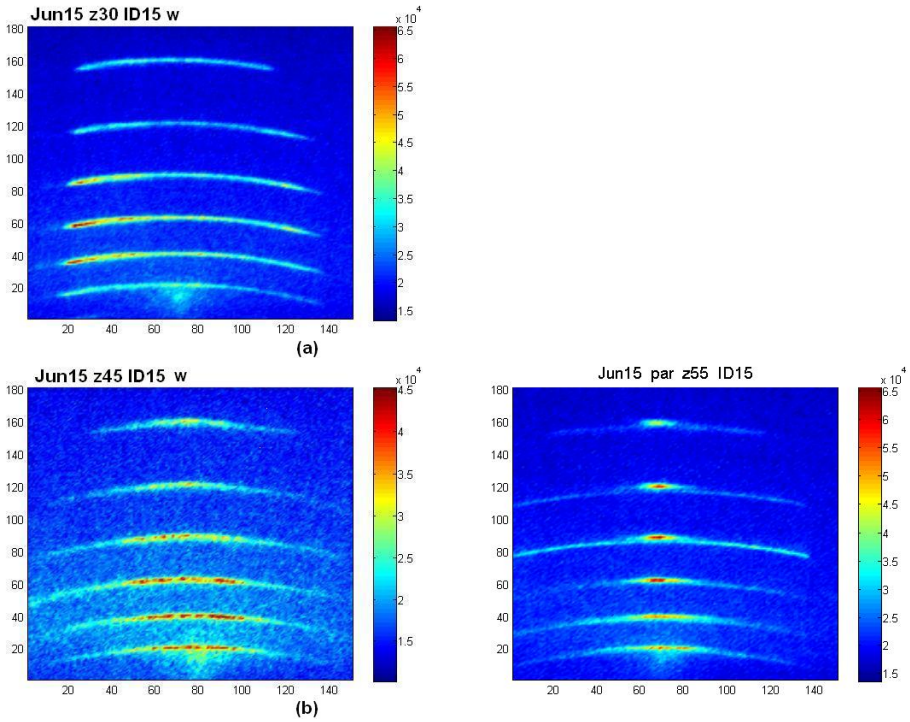

Figure 3.4: harmonic specrta of ω, ID 15 with distance of the parabolic mirror from the gas target (a) 30 mm , (b) 45 mm, (c) 55 mm

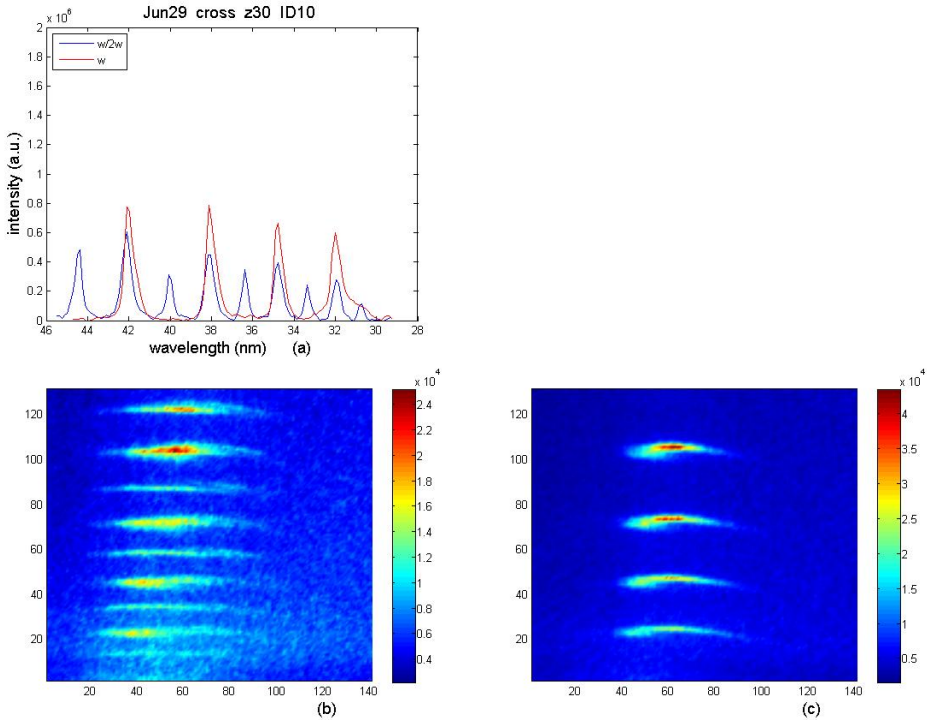

Figure 3.5: (a) specrta of ω and $\omega/2\omega$ harmonics, (b) color harmonic spectrum of the $\omega/2\omega$ beam, (c) color harmonic spectrum of the ω beam

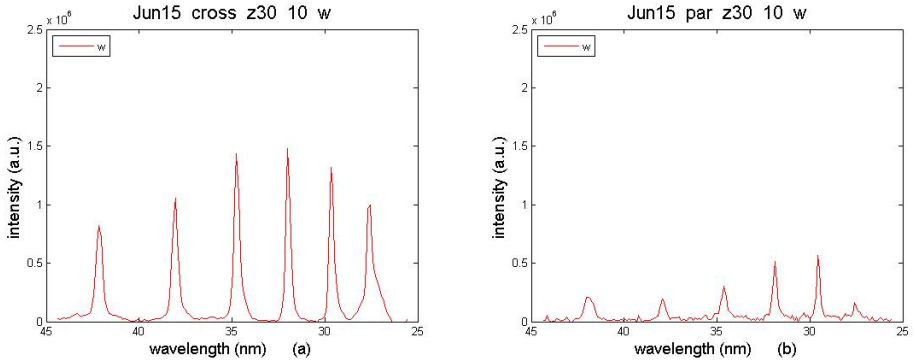

Figure 3.6: (a) spectrum of ω with crossed polarized beams, (b) specrtrum of ω with parallel polarized beam

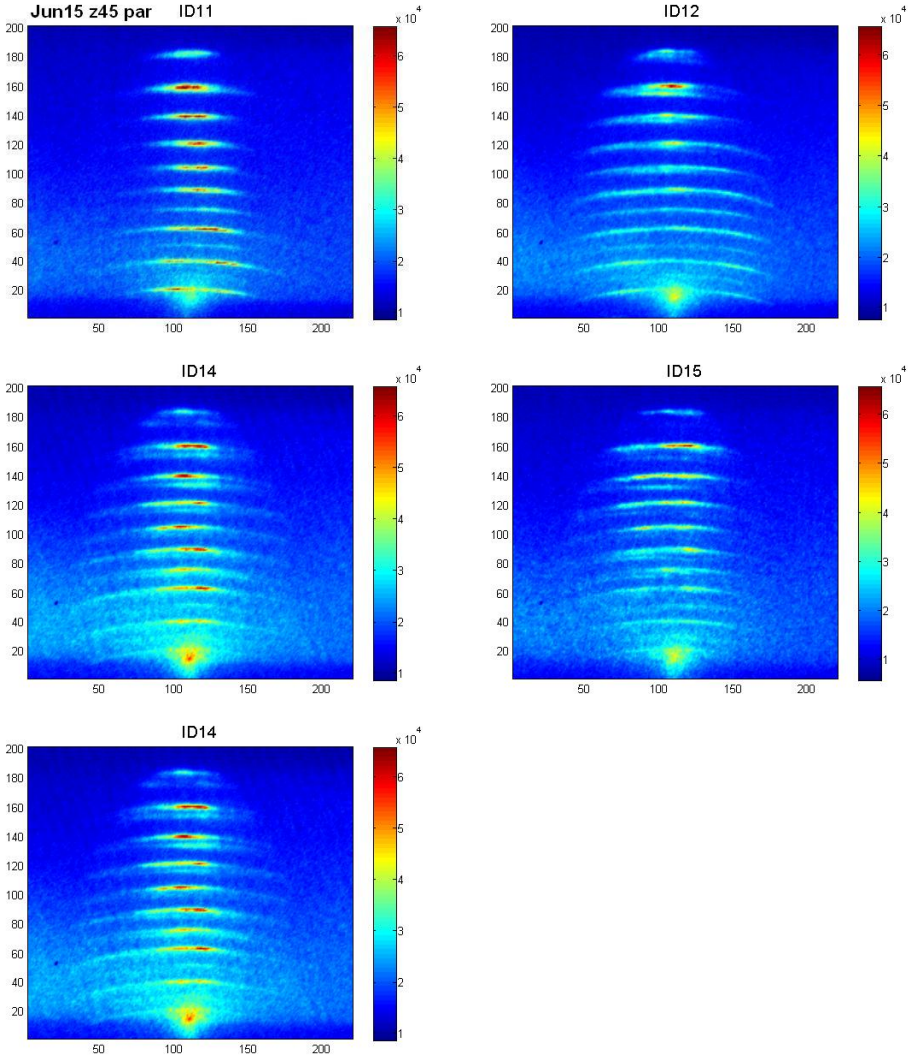

Figure 3.7: spectra taken under the same conditions, with different iris diameters (ID)

Chapter 4

Discussion and conclusions

A lot of data were generated, under different conditions, using ω and 2ω beams, separately and together. Here we try to interprete some of the results.

In general, enhancement of the harmonics is observed, when 2ω is added

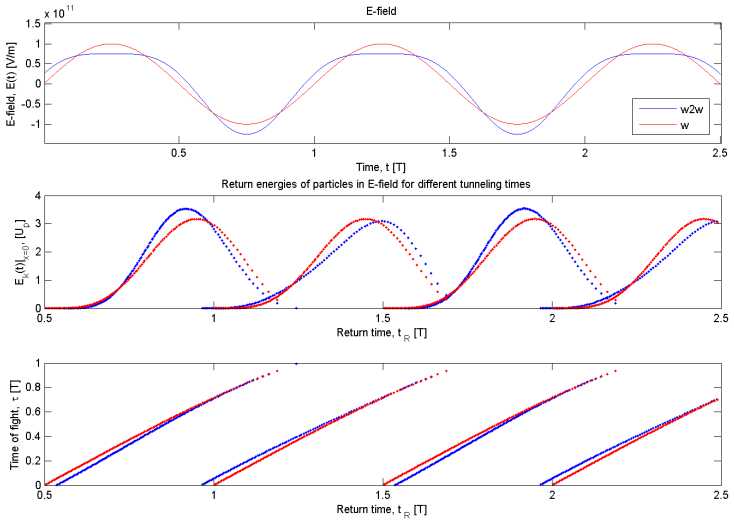

Figure 4.1: (a) Laser field, (b) return Energy, (c) time of flight

(see figure 3.1b, c). Divergence is another parameter that is changed when we use ω and 2ω beams together, as it is very clearly observed in figures 3.1 and 3.2, the harmonics $\omega/2\omega$ are wider than the ω ones. Double structure

is also observed in some cases, as it is shown in figure 3.8m. Effect that is becoming more strong as the beam is getting bigger (defined by Iris Diameter size).

According to the classical approach, depicted in figure 4.1, one can see that when the 2ω beam is added to the ω, the laser field enhances during the *tunneling* part of the first half of the period T. Fact that it is observed in the experimental data. Longer time of flight leads to more divergent harmonics in the $\omega/2\omega$ case, taking into consideration only the short trajectories, because the long ones will not show up in the measurements in a stable way. Such an example is very well depicted in figure 3.5, in which one clearly observe that the $\omega/2\omega$ harmonics (longer time of flight) are more divergent than the ω harmonics (shorter time of flight).
It has to be noted that only the half period with the intensisty peak is considered, because there is the highest and more significant number of electrons which are tunneling out.

In figure 4.1 plots with no delay between ω and 2ω are given, but similar results are produced even for delayed 2ω relative to ω (or the opposite), with small differences only in the return energy.

Finally, it was an interesting project through which an experimental setup was built leading to efficient $\omega/2\omega$ harmonic generation. Nice spectra were generated leading to interesting conclusions.

Appendix A

Programs

The simulation and analysis of the experimental data was done in MATLAB with the programs presented below, which can be found to the following site: *afbackup\ hhg\ Projects\ TUIXS\ Elisavet MATLAB programs*

1) spectrum.m
The whole spectrum is given in a pcolor plot with low order harmonics on top, according to the dimensions specified by the user in the beginning of the program, with counters in both axis x and y. Then a simple plot of this spectrum is created, with a counter in the x axis and intensity in the y axis. This plot enables the user to find the pixel corresponding to each harmonic, needed for the *lambda* (wave length in nm) *calibration* for this particular spectrum's data (generated in Excel).

2) final.m
The plot of the whole spectrum is given with wavelength (nm), taken from the particular *lambda calibration equation*, in the x axis and intensity (a.u.) in the y axis.
By choosing the points of the plot with the lower intensity, the program interpolates them and creates a background (noise) level which afterwards is deducted from the spectrum's intensity and a new *noise free* spectrum plot is created.
A figure with plots of separate harmonics is then created, whose dimensions are defined by the user in the program.
The last figure contains color plots of each harmonic presented in the previous figure, with counters in both axis, x and y.

3) final advanced.m
Two plots ($\omega/2\omega$ and ω) are given, with wavelength (nm) in x axis and intensity (a.u.) in the y axis. The noise is deducted as in the *final.m* and a

figure, of both *noise free* spectra plots, is generated with wavelength (nm) in x axis and intensity (a.u.) in the y axis.
Then a figure is created with two subplots, each one of a chosen, by the user, harmonic, by declaring the dimensions in the program.
The last figure shows color plots of the common harmonics (according to each one of the two data files, $\omega/2\omega$ and ω). Additionally, two more color plots of $\omega/2\omega$ harmonics are exposed, all of them with counters in both axis.

4) gauss fitting.m
A color plot of a chosen harmonic (harmonic dimensions are given by the user in the program) is created.
Then a plot of the particular harmonic is made with a counter in the x axis and intensity in the y axis, as well as a gauss fitting, which is presented in the same plot.

5) pcolor 1 harmonic.m
A color plot of 1 harmonic is generated, whose dimensions are given by the user in the program.

6) jun15 z30 10 final lamda.m
Two plots ($\omega/2\omega$ and ω) are given, with lambda (nm) in x axis and intensity (a.u.) in the y axis. The noise is deducted as in the *final.m* and a figure of both *noise free* spectra plots is generated with wavelength (nm) in x axis and intensity (a.u.) in the y axis.
The last figure gives color plots of the common harmonics (according to each one of the two data files, $\omega/2\omega$ and ω). Additionally, two more color plots of $\omega/2\omega$ harmonics are generated. All of them with *divergence* (in mrad) in x axis and *lambda* (in nm) in y axis.

STRAIGHTENING PRORAMS
1) straightening1.m and **2) straightening2.m**
In some cases the harmonic lines are coming quite "curvy" in the color spectrum plot. These programs 'straighten' the lines so that problems in integration are avoided. The procedure is the following:
1. Chose one 'curvy image' file, without any other effect, as for example double structure.
2. Open it with the *ImageJ* program and press the *polygon selections* button (3rd from the left). Click on the image, on one representive harmonic that you want to 'straighten' and then make a straight line as you want the harmonic to be (see example in figure A.1).
3. Save it as XY coordinates (it is saved then as a *.txt* file with the same name and in the same folder).

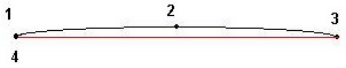

Figure A.1:

4. Go to the MATLAB program *straighening1.m*.
Change the path to the path of the *.txt* file you have just created and run it.
5. Write down the values of the constants R_o (radius), x_o and y_o (coordinates of the center of the suposed circle) that they appear in the command window.
6. Go to the MATLAB proram *straighening2.m*.
Change the existing R_o, x_o, y_o values to the values you have just written down, as well as the path name to the path of the folder, where the original image is.
7. *straighening2.m* program saves a new file (image) with straightened lines, adding the part *cor* in its name, keeping the rest of the name the same.

Appendix B

"lambda" calibration

From a simple plot of each spectrum, generated with *spectrum.m*, the following *wavelength (lambda) equations* are calculated, for the data files presented in this report. With these equations, the replacement of the x axis counter by wavelength (in nm) in the specta plots is possible, as well as the replacement of the y axis counter in the color plots of the spectra and of the separate harmonics, giving the user the possibility to find the precise wavelength of each harmonic (see figure 3.4).

The calculated lambda equations that were used in this report are given below:

1. Jun15 par z30 10 ($\omega/2\omega$), y = 0.1045x + 25.454, $R^2 = 0.9999$,
   harmonic orders from 29, 28,..., 19
2. Jun15 par z30 10 (ω), y = 0,1059x + 25.404, $R^2 = 0.9999$,
   harmonic orders from 29, 27,..., 19
3. Jun15 par z55 12 ($\omega/2\omega$), y = 0.1258x + 27.205, $R^2 = 0.9999$,
   harmonic orders from 27, 26,..., 16
4. Jun15 par z55 12 (ω), y = 0.1253x + 27.387, $R^2 = 1$,
   harmonic orders from 27, 25,..., 17
5. Jun15 cross z30 10 (ω), y = 0.1057x + 25.346, $R^2 = 0.9999$
   harmonic orders from 29, 27,..., 19
6. Jun29 cross z30 10 ($\omega/2\omega$), y = 0.1264x + 29.064, $R^2 = 0.9998$,
   harmonic orders from 26, 25,..., 18
7. Jun29 cross z30 10 (ω), y = 0.1245x + 29.025, $R^2 = 0.9999$,
   harmonic orders from 25, 23,..., 19

Appendix C

General instructions for the experiments

1. Align the setup (many times if needed)

2. Put the spectrometer and the gas jet under vacuum (section 2.4)

3. Turn on the Argon gas (orange bottle)
First the silver and then the black to *2mbars* - right indicator.

4. Empty the box (on the table, behind the gas buffer)
Watch the pressure in the right indicator (≈ 0) and turn it off, the Ar comes.

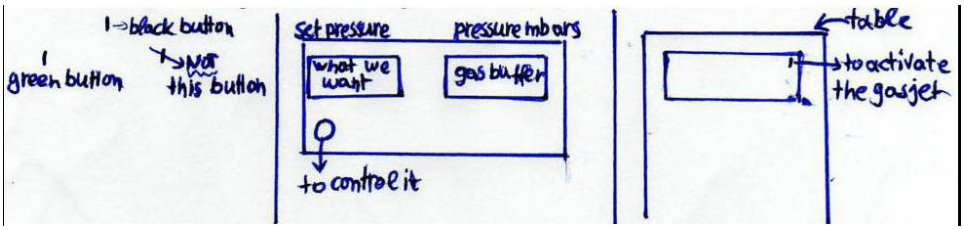

Figure C.1:

5. Check theat everything is closed before putting the gas jet under vacuum.
6. First turn on 1 (with the back button).
If 2 is not at $p = 10^{-1}$, turn it on, with the switching on button and when $p < 10^{-1}$, turn ON the turbo (box to the right of the PC).

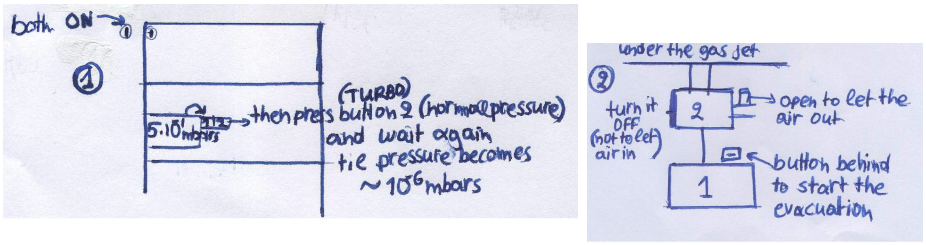

Figure C.2:

7. The same to be done under the detector (and spectrometer). The pressures sould be more or less the same to let the gas go to the detector. The pressure under the detector has to be, though, a little bit smaller than the pressure of the gas.
8. Empty the gas jet first, before refilling it again.
9. Pumping
   1 has to closed
   2 has to be open
   Then tunn it ON (button behind the white box).

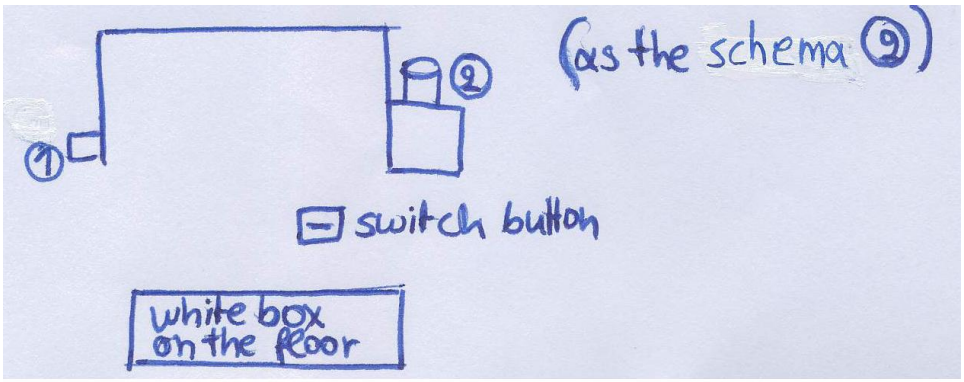

Figure C.3:

MCP Voltage

1. First turn ON the button down to the right.
2. Zero the small screen in the middle.
3. Turn ON the buton down to the left.
4. Inrease the number 1 with step of 100 until it reaches the 1000
   Then do the same with the number 2 (step 100 till the 1000)
   Then increase the number 1 again, with step of 100 until it reaches the 3000.
   In the end increase the 2 with step of 100 till 1570).

Exposure time: 60000
Control
No of samples: 40 (click on the *Remote* buton,beside the *Acquire* button)
To work, click on the *Live* button
When you stop the files are saved in a temporary folder.

ImageJ
Ploggins
Edit
macros → openspectrum.txt
here you give the name you want to the file
save pathname → change it
maros → openspectrum

Create a folder with the name you want (the one that you have used for the path in the openspectrum.txt)

Bibliography

[1] A. L'Huillier, O.Guilbaud, E. Georgiadou, B. Schütte, G. Genoud, E. Mengotti, E. Pourtal, J. Mauritsson, Spatial and spectral properties of high order harmonic generation for X-ray laser seeding, Poster on the frame of the TUIXS General Meeting, Lisbon, Instituto Superior Técnico, May 2006

[2] A. L'Huillier, Atoms in strong laser fields - Generation of attosecond pulses, Laboratory exercice, Advanced Atomic Physics, 2004

[3] L. Roos, Optimisation and Application of Intense High-Order Harmonic Pulses, Lund Reports on Atomic Physics, LRAP-276, Lund University, August 2001

[4] B. Schütte, Optimization of High-order Harmonic Generation using an Ultrashort Pulse High-Intensity Laser, Lund Reports on Atomic Physics, LRAP-360, Lund University, May 2006

[5] E. Mengotti, G. Genoud, Towards Time-Resolved X-UV Digital in-line Holography, Lund Reports on Atomic Physics, LRAP-368, Lund University, September 2006

[6] T. Eberle, J. Klemmer, Design, Construction and Study of a new Gas Target for High-Order Harmonic Generation, Lund Reports on Atomic Physics, LRAP-371, Lund University, January 2007

[7] J. Levesque, D. Zeidler, J.P. Marangos, P.B. Corkum and D.M. Villeneuve, High Harmonic Generation and the Role of Atomic Orbital Wave Functions, July 2006

[8] P. Balcou, R. Haroutunian, S. Sebban et al., High-order harmonic generation: towards laser-induced phase-matching control and relativistic effects, Appl Phys.B74, 509-515 (2002)

[9] J. Mauritsson, P. Johnsson, E. Gustafsson, A. L'Huillier, K. J. Schafer, and M.B. Gaarde, Attosecond Pulse Trains Generated Using Two Color Laser Fields, Phys. Rev. Lett. 97, 013001 (2006).

[10] S. Kazamias-Moucan, Optimisation d'une source d'harmonique d'ordre levs pour l'optique non-linaire dans l'extrme UV, PhD thesis, Ecole Polytechnique, 2003.

[11] O. Guilbaud, B. Schütte, E. Georgiadou, E. Pourtal, and A. L'Huillier, Spectral control of high-order harmonics.

[12] I.J. Kim, C. M. Kim, H.T. Kim, G.H. Lee, Y.S. Lee, J.Y. Park, D.J. Cho, and C.H. Nam, Highly Efficient High-Harmonic Generation in an Orthogonally Polarized Two-Color Laser Field, Phys. Rev. Lett. 94, 243901 (2005).

[13] O. Guilbaud, E. Mengotti,G. Genoud, N.Adie, S.G.Pattersson, E. Georgiadou, E. Pourtal, C.G. Wahlström and A. L'Huillier, Digital in line holography using High Harmonic.

[14] C. *Lyngå*, High-Order Harmonics Characterization, Optimization and Application, PhD Thesis, Lund Institute of Technology, LRAP-276, 2001..

[15] P. Johnsson, Attosecond Optical and Electronic Wave Packets,PhD thesis, Lund University, 2006

[16] F. Lindner, W. Stremme,M.G. Schätzel, F. Grasbon, G.G. Paulus, H. Walther, R. Hartmann and L. Strüder, High-order harmonic generation at a repetition rate of 100kHz, Phys. Rev. A 68, 013814, 2003